

High-Current Betatron with Stellarator Fields

C. W. Roberson

Office of Naval Research, Arlington, Virginia 22217

and

A. Mondelli

Science Applications, Inc., McLean, Virginia 22102

and

D. Chernin

Berkeley Research Associates, Springfield, Virginia 22150

(Received 2 November 1982)

By adding an $l=2$ stellarator field to a betatron accelerator, a new configuration is obtained which is capable of accelerating multikiloamp beams and which will tolerate a large (more than 50%) mismatch between the particle energy and the vertical magnetic field. The additional field is a twisted quadrupole which acts as a strong-focusing system. This device has been analyzed both analytically and numerically.

PACS numbers: 52.75.Di, 29.20.Fj

Conventional betatrons^{1,2} are current limited at injection. Recently, efforts have been made to extend the current-carrying capability of the betatron. For example, the plasma betatron³ employs a toroidal magnetic field in the direction of the particle orbit to contain the plasma. Current interest is focused on high-current nonneutral electron acceleration in modified betatrons.⁴⁻⁶

By adding a stellarator field to a cyclic accelerator, a strong-focusing system⁷ is obtained which can sustain high currents and large mismatch between particle energy and vertical field. The energy bandwidth relaxes the design requirements for the injector and the magnetic field system. Unlike fixed-field alternating-gradient betatrons,⁸ the stellarator-betatron (or stellatron) includes a strong toroidal field to confine very high currents. Figure 1 shows a sketch of the stellatron configuration.

We have quantitatively studied the stellatron configuration. Our studies have consisted of numerical and single-particle orbit calculations, as well as analytical linearized orbit theory, including the beam self-fields.

We may study the behavior of an intense electron beam in the stellatron quantitatively by considering small departures from a "reference orbit," a circle located at the null point in the quadrupole field, at $r=r_0$, $z=0$. Here and below we use a cylindrical (r, θ, z) coordinate system with origin at the center of the torus's major cross section. Quantities evaluated at the reference orbit will carry a subscript 0 below; departures from this orbit will carry a subscript 1.

The twisted quadrupole field, of period $2\pi/m$, then is written as

$$\begin{aligned} B_r &\cong kB_s(-r_1 \sin m\theta + z_1 \cos m\theta), \\ B_z &\cong kB_s(r_1 \cos m\theta + z_1 \sin m\theta), \quad B_\theta \cong B_{\theta 0}, \end{aligned} \quad (1)$$

where $k, B_s, B_{\theta 0}$ are constants, and the betatron field is

$$B_r \cong -nB_{z0}z_1/r_0, \quad B_z \cong B_{z0}[1 - n(r_1/r_0)], \quad (2)$$

where B_{z0} is the vertical field at the reference orbit and n is the usual field index.

We consider the motion of an electron located within a beam whose center is located at $r=r_0 + \Delta r$, $z=\Delta z$; the electron's position is $r=r_0 + \Delta r + \delta r \equiv r_0 + r_1$, $z=\Delta z + \delta z \equiv z_1$. Using a cylindrical approximation for the beam self-fields, we

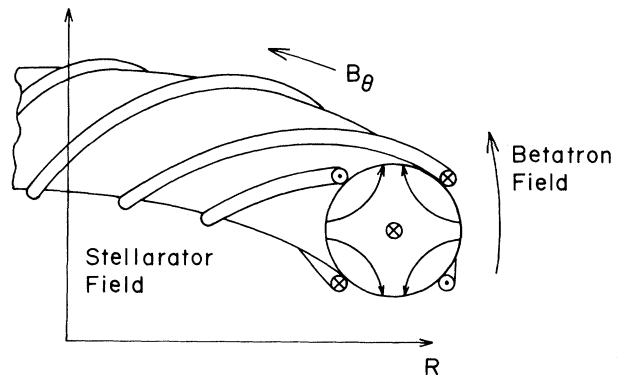


FIG. 1. Stellatron configuration.

find

$$\ddot{r}_1 + \Omega_{z_0}^2(1 - n + \mu \cos m\theta)r_1 - \frac{1}{2} \frac{\omega_b^2}{\gamma_0^2} \left(\delta r + \frac{r_b^2}{a^2} \Delta r \right) = \frac{\gamma_1 c^2}{\gamma_0 r_0} - (\mu \Omega_{z_0}^2 \sin m\theta)z_1 + \Omega_{\theta_0} \dot{z}_1, \quad (3a)$$

$$\ddot{z}_1 + \Omega_{z_0}^2(n - \mu \cos m\theta)z_1 - \frac{1}{2} \frac{\omega_b^2}{\gamma_0^2} \left(\delta z + \frac{r_b^2}{a^2} \Delta z \right) = -(\mu \Omega_{z_0}^2 \sin m\theta)r_1 - \Omega_{\theta_0} \dot{r}_1, \quad (3b)$$

$$\dot{\theta}_1 = -(r_1/r_0)\Omega_{z_0}, \quad (3c)$$

where $\Omega_{z_0} = eB_{z_0}/m\gamma_0 c$, γ_0 is the relativistic factor for the reference orbit, $\omega_b^2 = 4\pi n_0 e^2/m\gamma_0$, n_0 is the beam number density, r_b is the minor radius of the beam, a is the minor radius of the (perfectly conducting) chamber, and $\mu = kr_0 B_s/B_{z_0}$.

By performing a formal ensemble average of (3a)–(3c) one may find equations governing single-particle motion and that of the beam centroid. Details will be published elsewhere. By changing the independent variable from t to θ , and making the transformation $\xi = (r_1 + iZ_1)/r_0 = \psi \exp(im\theta/2)$, one obtains an equation for ψ which may be solved in the special case, $n = \frac{1}{2}$, with the following results.

Particle motion is oscillatory (under certain conditions; see below) about a center located at

$$\frac{\delta r}{r_0} = \frac{\Delta - \langle \Delta \rangle}{\bar{n}_p + \mu^2(m^2 + mb - \bar{n}_p)^{-1}}, \quad (4)$$

where $\bar{n}_p = \frac{1}{2} - n_s$, $n_s = \omega_b^2/2\gamma_0^2\Omega_{z_0}^2$, $b = B_{\theta_0}/B_{z_0}$, $\Delta = \gamma_1/\beta_0^2\gamma_0$, and angular brackets denote an ensemble average. There are five characteristic oscillation frequencies, $m\Omega_{z_0}$ and $(m/2 \pm \nu_{\pm})\Omega_{z_0}$, where

$$\nu_{\pm}^2 = \hat{n} + \frac{1}{4}\hat{m}^2 \pm (\hat{n}\hat{m}^2 + \mu^2)^{1/2} \quad (5)$$

with $\hat{n} = \bar{n}_p + \frac{1}{4}b^2$, $\hat{m} = m + b$. These frequencies are real when the system is located within the regions of the plane of Fig. 2 marked "stable." We remark that for low-current beams ($n_0 \rightarrow 0$) the stability condition reduces to

$$|\frac{1}{2}m^2 + mb - 1| > |2\mu|. \quad (6)$$

The "most" stable configuration results when the field lines are twisted clockwise ($m > 0$) when viewed in the direction of $B_{\theta_0}\hat{\theta}$, i.e., in the same sense as electron gyration about B_{θ_0} .

Similarly, the motion of the beam center is itself oscillatory about a center located at

$$\frac{\Delta r}{r_0} = \frac{\langle \Delta \rangle}{\bar{n}_b + \mu^2(m^2 + mb - \bar{n}_b)^{-1}}, \quad (7)$$

where $\bar{n}_b = \frac{1}{2} - (r_b^2/a^2)n_s$, with characteristic frequencies as in (5), under the replacement $n_s \rightarrow (r_b^2/a^2)n_s$.

Two important features of the solution are worth

pointing out. First, stable motion is possible throughout an injection-acceleration cycle. This has been checked for many possible time histories. A typical trajectory in the stability plane is shown in Fig. 2. The unstable region on the left of the diagram would not be entered in this case even if the acceleration were continued; "u" never changes sign in this case.

The second important feature of the solution pertains to the energy bandwidth of this machine. We note that the radial shift (7) of the orbit of a mismatched beam is, as expected, much smaller than that in a weak focusing ($\mu = 0$) device. (μ can easily exceed 100–200 in designs we have considered.) The stellerator's large energy bandwidth has very helpful consequences for injector and magnetic field design tolerances.

The introduction of *fixed* toroidal and helical fields to the betatron causes the betatron wavelengths to depend on energy, resulting in resonant instabilities driven by field errors during acceleration. If the toroidal field is sufficiently large, the betatron wavelengths will be insensitive to beam current. Such instabilities may be avoided by holding all the fields in constant ratio during acceleration. Alternatively, the effect of the

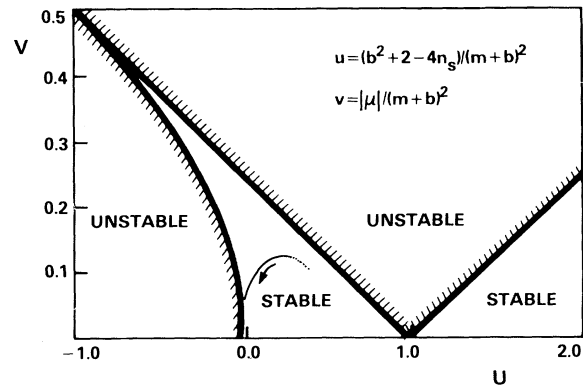


FIG. 2. Stellerator stability plane ($n = \frac{1}{2}$). The dotted line is the trajectory of an experiment with $I = 10$ kA, $B_{\theta_0} = 5$ kG, $\epsilon_1 \equiv 2\mu/mb = 1$, $m = 20$, $r_0 = 1$ m, while B_{z_0} is raised from 118 to 1700 G, corresponding to an increase in energy from ~ 3.5 to 50 MeV.

instabilities may be minimized if the energy gain per revolution is large enough to pass rapidly through each resonance.

A single-particle code, which integrates the relativistic equations of motion for an electron in an applied magnetic field, has been utilized to study certain nonlinear aspects of the stellatron configuration. Unlike the analytical analysis of the preceding paragraphs, this analysis does not employ a paraxial approximation for the electron motion and does not use an expansion in the particle displacement from a reference orbit. Also, the applied field in this analysis includes toroidal corrections to first order in the inverse aspect ratio.

The total magnetic field utilized by the code may be expressed as $\vec{B} = \vec{B}_b + \vec{B}_s$, where \vec{B}_b is the conventional betatron field, given by Eq. (2), and \vec{B}_s is the stellarator field, given by $\vec{B}_s = \nabla\Phi_s$, in terms of the magnetic scalar potential, Φ_s , which may be expressed as $\Phi_s^{(0)} + \Phi_s^{(1)}$, where

$$\Phi_s^{(0)}(\rho, \varphi, s) = B_{\theta 0} \{ s + (\epsilon_l / \alpha) I_l(x) \sin[l(\varphi - \alpha s)] \}.$$

Here, $x = l\alpha\rho$, $\alpha = 2\pi/L$, L is the helix pitch length, and I_l represents the modified Bessel function. The coordinates (ρ, φ, s) form a local cylindrical system centered on the minor axis, where $s = R_0\theta$ is distance measured along the minor axis for toroidal angle θ , and (ρ, φ) are polar coordinates in the plane transverse to the

minor axis at s . The toroidal correction, $\Phi_s^{(1)}$, is given to first order in the inverse aspect ratio by Danilkin.⁹ All calculations have been performed for $l=2$. The variables μ and m , which describe the helical field in the previous analytical analysis, are given by $\mu = \epsilon mb/2$ and $m = 2\alpha R_0$ for $l=2$.

This model has been utilized to investigate the single-particle bandwidth of the stellatron. As ϵ_l increases, the allowed mismatch in the stellatron becomes too large to be correctly modeled by the linearized theory. Figure 3 shows the results from both models for bandwidth versus ϵ_l . These calculations assume a torus having a 1-m

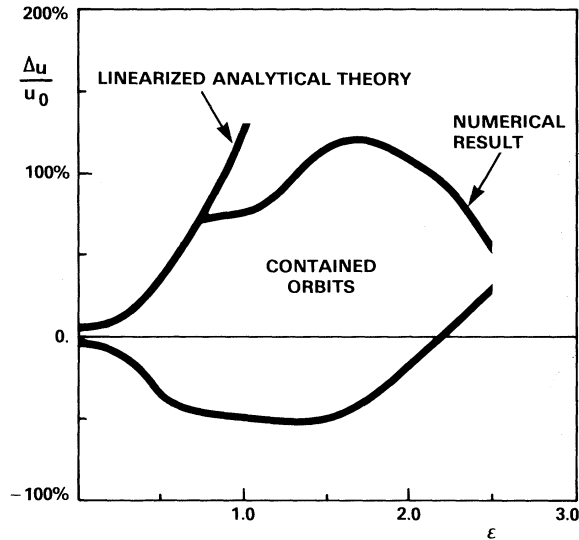


FIG. 3. Stellatron single-particle bandwidth. The bandwidth $\Delta u/u_0$, where $u = \gamma\beta$, is plotted against $\epsilon_l \equiv 2\mu/mb$. The accelerator is matched at $\gamma=7$ with $B_{z0} = 118$ G, and $B_{\theta 0} = 1$ kG.

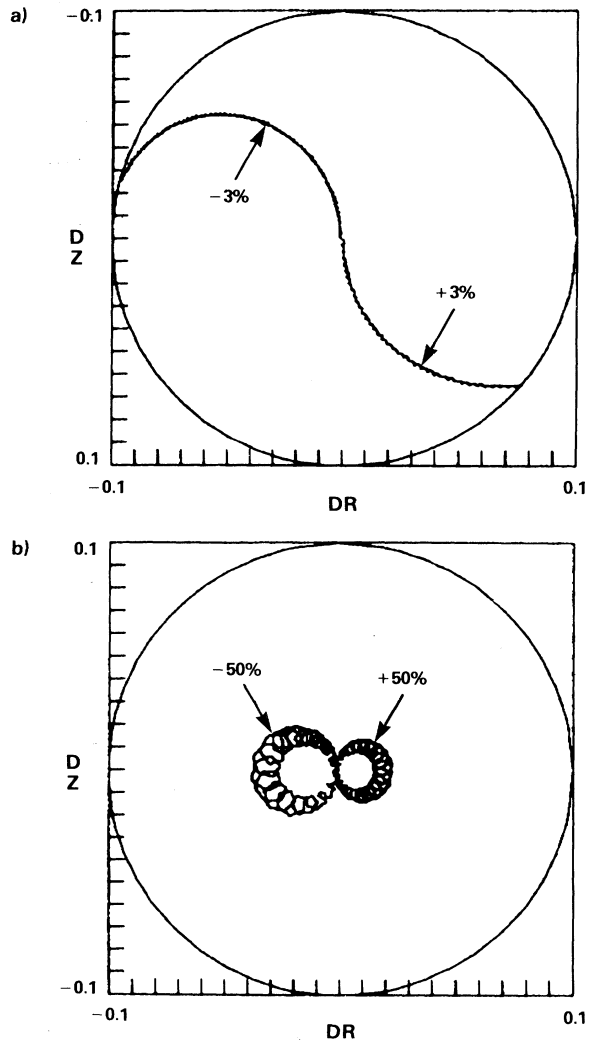


FIG. 4. Single-particle orbits. (a) Without the helical field components ($\epsilon_l \equiv 0$), $\Delta u/u_0 = \pm 3\%$; (b) stellatron orbit with $\epsilon_l = \frac{1}{2}$, $\Delta u/u_0 = \pm 50\%$.

major radius and a 10-cm minor radius. A test electron is launched tangent to the minor axis with relativistic momentum $u = \gamma\beta$, which differs from the matched momentum, u_0 , by varying amounts, Δu . The figure shows $\Delta u/u_0$ against ϵ_1 , and represents the maximum $|\Delta u/u_0|$ for which the test orbit remained confined in the device. Mismatch in excess of 50% can be tolerated for these parameters.

Figure 4(b) shows typical stelleron orbits, projected on the minor cross section, for $B_{\theta 0} = 5$ kG, $\epsilon_1 = \frac{1}{2}$ for $\pm 50\%$ mismatch. The betatron field is again 118 G with $n = \frac{1}{2}$. Without the helical field contribution, Fig. 4(a) shows that as little as $\pm 3\%$ mismatch is not tolerable.

The superposition of twisted quadrupole, toroidal, and conventional betatron magnetic fields appears to offer significant practical advantages for the confinement and acceleration of large electron currents (tens of kiloamperes) to moderate energies (hundreds of megaelectronvolts). Foremost among these advantages is the greatly improved energy bandwidth over that of a weak-focusing device. The large bandwidth of the stelleron relaxes the requirements for monoenergetic injection, for a uniform (within a few percent) magnetic field configuration, and for a rigid mechanical design. Injection should not be any more difficult than for other high-current accelerator concepts, and is facilitated by the externally applied rotational transform of the stelleron field. The orbits should remain stable

from injection up to the highest energies achievable by conventional inductive acceleration.

It is a pleasure to acknowledge numerous discussions with members of the Naval Research Laboratory Special Focus Program "Advanced Accelerators." This work was supported by the Naval Research Laboratory.

¹D. W. Kerst, Phys. Rev. **58**, 841 (1940).

²D. W. Kerst, G. D. Adams, H. W. Koch, and C. S. Robinson, Phys. Rev. **78**, 297 (1950).

³L. A. Ferrari and K. C. Rogers, Phys. Fluids **10**, 1319 (1967).

⁴P. Sprangle and C. A. Kapetanacos, J. Appl. Phys. **49**, 1 (1978).

⁵N. Rostoker, Comments Plasma Phys. Controlled Fusion **6**, 91 (1980).

⁶P. Sprangle, C. A. Kapetanacos, and S. J. Marsh, in Proceedings of the International Topical Conference on High-Power Electron and Ion Beam Research and Technology, Palaiseau, France, 1981 (unpublished), p. 803.

⁷A. A. Mondelli and C. W. Roberson, NRL Memorandum Report No. 5008, 1982 (unpublished).

⁸K. R. Symon, D. W. Kerst, L. W. Jones, L. J. Laslett, and K. M. Terwilliger, Phys. Rev. **103**, 1837 (1956).

⁹I. S. Danilkin, in *Stellarators*, Proceedings of the P. N. Lebedev Physics Institute, edited by D. V. Skobel'tsyn (Consultants Bureau, New York, 1974), Vol. 65, p. 61ff.